ELSEVIER

Chemical Engineering Journal 83 (2001) 15–23

Chemical Engineering Journal

www.elsevier.com/locate/cej

Application of branched pore diffusion model in the adsorption of reactive dyes on activated carbon

Xiao-Yan Yang, Bushra Al-Duri*

School of Chemical Engineering, University of Birmingham, Edgbaston, Birmingham B15 2TT, UK

Received 30 July 1999; received in revised form 27 June 2000; accepted 12 July 2000

Abstract

In this work, the branched pore diffusion model (BPDM) was applied to the single component adsorption of three reactive dyes on activated carbon in a batch stirred vessel. Results are in terms of theoretical concentration decay curves, characterised by the non-linear combination of four mass transfer parameters namely the external mass transfer coefficient k_f, the solid diffusivity D_s, the micropore rate coefficient k_b and the fraction micropores *f*. An 'improved' solution technique was presented where an optimising subroutine was employed to select 'best' combination of the mass transfer parameters. Compared to the existing methods, this yielded more accurate results over a longer period of adsorption and shorter computational time. Also, equilibrium was accurately described by the Fritz–Schlünder isotherm. Results showed that, over a wide range of system conditions, a single k_f, k_b and *f* value described each dye/carbon system; while D_s increased with the initial solution concentration, C_0. Furthermore, D_s was mathematically related to the surface loading q_s. This paper provides an in-sight into the relation between the sorbent surface, the solute properties and the adsorptive characterictics.

Keywords: Adsorption; Branched pore diffusion model; Fritz–Schlünder isotherm; Kinetics; Mass transfer parameters; Numerical solution

1. Introduction

Adsorption is an efficient and economically feasible process for the treatment of wastewater containing chemically stable pollutants. Reactive dyes are of the most common dyes used due to their advantages, such as operating under mild conditions and bright colours [1]. As most reactive dyes are hydrolysed to some extent during application (to cellulose fibres for instance), some of the reactive dyestuff is inactivated by a competing hydrolysis reaction. This results in unfixed hydrolysed dyestuff in the water and produces unacceptable levels (10–50% of the initial dye), of colour in mill effluents [2]. Also, reactive dyes are chemically stable and are therefore inadequately treated by the conventional treatment works.

For the purpose of flexible and theoretically sound design of adsorption columns, various adsorption models have been proposed over the years for the theoretical prediction of adsorption kinetics. However, the branched pore diffusion model (BPDM) proposed by Peel et al. [3], is the only model (to date) which incorporates the internal structure of the adsorbent into the theoretical description of adsorption kinetics. It simplifies the poly-disperse structure of activated carbon into two pore-size regions; namely macropores [$d_p > 200$ nm] and micropores [$d_p < 200$ nm]. Intraparticle diffusion hence occurs by a dual mechanism: solute transports in the macropores by solid diffusion, followed by multidirectional interactions in the micropores. This explains the slow approach to equilibrium (in the micropores), and provides the theoretical description of system kinetics up to 72 h, which is not described by any other adsorption model. However, the complexity of the dual mechanism requires four mass transfer parameters to describe, in addition to extended computational time and tedious 'trial and error' method, in order to evaluate these parameters. For instance, it was found that 8 min were required to yield kinetic data for 9 h adsorption period for basic dyes on activated carbon, while 11 h were consumed to produce kinetic data for a contact time of 24 h [4].

Restricted by mathematical inconvenience, previous applications of the BPDM to phenol [3], basic dyes [4], metal cyanides [5] and in-pulp on activated carbon [6], and acid blue/chitin [7] systems, all presented a single set of mass transfer parameters, to describe the whole operating range. The accuracy of results depended on the system investigated.

The present work employed the solution method of McKay et al. [7], and added an optimising subroutine to

* Corresponding author. Tel.: +44-121-414-3969; fax: +44-121-414-5324.
E-mail address: b.al-duri@bham.ac.uk (B. Al-Duri).

1385-8947/01/$ – see front matter
PII: S1385-8947(00)00233-3

Nomenclature

a_s	Fritz–Schlünder isotherm parameter $(mg/l)^{-b_2}$
A	total interfacial surface area (m^2)
b_1, b_2	Fritz–Schlünder isotherm parameters (dimensionless)
Bi_f	modified film Biot number, $k_f C_0 R/\rho_c f D_s q_0$
C	liquid-phase concentration (mg/l)
C_s	liquid-phase concentration at outer surface of carbon particles
C_0	initial liquid-phase concentration (mg/l)
D_s	surface diffusivity (cm^2/s)
D_{s0}	parameter defined in Eq. (7) (cm^2/s)
f	fraction of total adsorptive capacity in macropores
ΔH_{st}	isosteric heat of adsorption (kJ/mol)
k	parameter defined in Eq. (7)
k_b	branch pore rate coefficient (s^{-1})
k_f	external liquid film mass transfer coefficient (m/s)
k_s	Fritz–Schlünder isotherm parameter $(mg/g)(mg/l)^{-b_1}$
N	number of points on an experimental curve
q	solid-phase concentration (mg/g)
q_0	solid-phase concentration in equilibrium with C_0
r	radial position inside the particle (cm)
R	adsorbent particle radius (cm)
R_b	micropore diffusion rate (mg/(g min))
R_g	ideal gas constant (kJ/(mol K))
t	time (s)
T	temperature (K)
V	liquid-phase volume (cm^3)
W	mass of activated carbon (g)

Greek letters

ρ_c	carbon particle density (g/cm^3)

Subscripts

b	micropore
cal	model-computed value
e	equilibrium value
exp	experimental value
m	macropore
sat	value at surface saturation

search for the best combination of mass transfer parameters. This greatly reduced the computational time from hours to minutes, and saved the effort associated with manual 'trial and error' work. Furthermore, it developed an exponential $q_s - D_s$ correlation out of the BPDM, not presented in previous works. The systems under investigation are reactive red (RR), reactive yellow (RY) and reactive navy (RN) on activated carbon F-400 in their single component systems.

2. Experimental

2.1. Material/analytical methods

All experiments were conducted using Filtrasorb-400 (F-400) activated carbon (Calgon, Pittsburgh, PA). Prior to its use, the activated carbon was crushed and screened to a series of particle sizes and then washed thoroughly in distilled water to remove fines. Afterwards it was dried at 110°C for 24 h. The accurate particle diameter was determined by image analysis of more than 200 particles for each particle size range.

RY, RR and RN supplied by Ciba Geigy were selected as adsorbates. All aqueous solutions were prepared in distilled water. Their concentrations were measured using an UV–Visible spectrophotometer (Cecil Instruments, Cambridge) at their respective optimum wavelengths namely 413, 537 and 597.2 nm for RY, RR and RN, respectively. All samples were filtered through a 0.45 μm membrane filter paper (Whatman International, Maidstone) before measurement in order to remove the carbon fines in it. The structure, type and number of functional groups in each dye are given in Appendix A.

2.2. Equilibrium studies

The equilibrium isotherms for RR, RY and RN adsorption on F-400 were determined at 25°C. For each reactive dye a set of dye solutions of consecutively increasing concentrations were prepared and brought into contact with pre-weighted amounts of carbon in at least 20 conical flasks. These flasks were then capped and put into a shaker, with temperature set at 25°C and the shaking speed set at 200 rpm. The liquid concentrations were measured after 25 days.

2.3. Kinetic studies

Kinetic studies were carried out in a 3 l glass vessel. The vessel was equipped with six stainless steel baffles distributed evenly around the circumference, and a sampling port with a rubber septum, which allowed for the withdrawal of samples from a fixed point near the centre of the vessel without interrupting the experiments. A six-flat-blade impeller, driven by a Heidolph electric motor (Heidolph-Elektro GmbH, KG, Kelheim) stirred the solution. Fig. 1 shows the schematic diagram and the dimensions of the batch reactor are given in Table 1.

3. Description of the branched pore diffusion model

The BPDM describes the adsorption mechanism as follows:

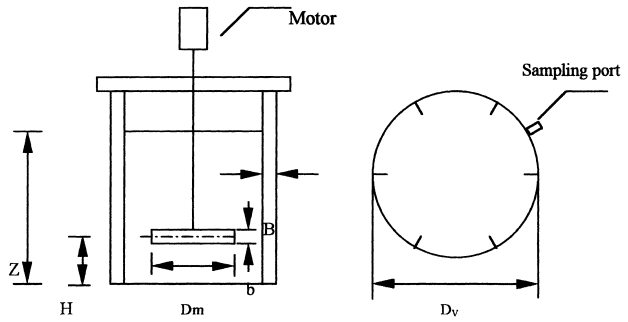

Fig. 1. Finite-bath (batch) reactor.

Table 1
Dimensions of adsorption batch reactor

Symbol	Description	Dimensions (cm)
Z	Height of liquid	15.1
D_v	Diameter of batch reactor	14.5
B	Width of baffles	1.45
H	Height of impeller	5.00
D_m	Impeller diameter	6.50
b	Width of blade of impeller	1.30

1. Film transfer from the solution bulk to the sorbent particle surface, measured by the external mass transfer coefficient k_f (cm/s):

$$V\frac{dC}{dt} = -k_f A(C - C_s) \quad (1)$$

2. Intraparticle diffusion in the macropores, described by solid diffusion (the surface hopping mechanism [8]). It is measured by the surface diffusivity D_s (cm^2/s):

$$f\frac{\partial q_m}{\partial t} = f\frac{D_s}{r^2}\frac{\partial}{\partial r}\left(r^2\frac{\partial q_m}{\partial r}\right) - R_b \quad (2)$$

3. Micropore diffusion described by multidirectional interactions between the pore walls and solute molecules. Its rate is monitored by the micropore rate coefficient, k_b (s^{-1}).

$$(1-f)\frac{\partial q_b}{\partial t} = k_b(q_m - q_b) = R_b \quad (3)$$

4. Eqs. (2) and (3) introduce a fourth parameter f, which represents the fraction of total adsorptive capacity in macropores, and $(1-f)$ represents the fraction of total adsorptive capacity in micropores.

Equilibrium exists between the solid- and liquid-phase solute concentrations at the interface. It is described by the Fritz–Schlünder formula [9]:

$$q_s = \frac{k_s C_s^{b_1}}{1 + a_s C_s^{b_2}} \quad (4)$$

The initial and boundary conditions are as follows:

$$q_m(r,0) = 0, \qquad q_b(r,0) = 0, \qquad C(0) = C_0,$$
$$q_m(R,t) = q_s(t), \qquad \frac{\partial q_m}{\partial r}(0,t) = 0,$$
$$k_f(C - C_s) = fD_s\rho_c\frac{\partial q_m}{\partial r}|_{r-R}$$

4. Solution method

This work adopts the numerical solution developed earlier by McKay et al. [7]. However, the programme was modified and improved in two aspects:

1. As mentioned earlier, it described equilibrium by the Fritz–Schlünder isotherm. The latter describes data more accurately for all liquid concentration ranges (Figs. 2–4).
2. An optimising subroutine E04JAF was downloaded from NAG Fortran Library to search for the *best combination* of mass transfer parameters. Data from literature were used as guideline to decide the starting range of the values for the four parameters. Iteration followed to select more accurate set of parameters.

This improvement resulted in an accurate description of system kinetics over longer periods of operation, in a much shorter computational time. Furthermore, it enabled the model to produce variable D_s values, without mathematical inconvenience. This is a novelty that had not been achieved in previous literature.

5. Results and discussion

5.1. Equilibrium isotherm

Equilibrium behaviour of an adsorption system is an essential requirement for modelling of system kinetics. A clear review of the various equilibrium isotherms and their applications is in literature [10]. The Fritz–Schlünder isotherm selected for this work, is a hybrid between the Langmuir and the Freundlich. In other words, it contains the heterogeneity factors (b_1 and b_2) that account for the sorbent heterogeneity on the one hand, and shows a high degree of irreversibility, which characterises diffusion in the micropores, on the other hand. Therefore, the selected isotherm described the current data with high degree of accuracy over a wide concentration range (Figs. 2–4).

The k_s/a_s values and the q_{sat} values for the three dyes in Table 2 reveal that activated carbon F-400 had a greater affinity (or capacity) for RY than for RR and RN. Appendix A shows that RY has a smaller size and lower polarity (smaller number of polar functional groups) than RR and RN, the reason why RY was more strongly adsorbed. On the other hand, the molecular structures and polarity of RR and RN are much similar to each other, hence they showed

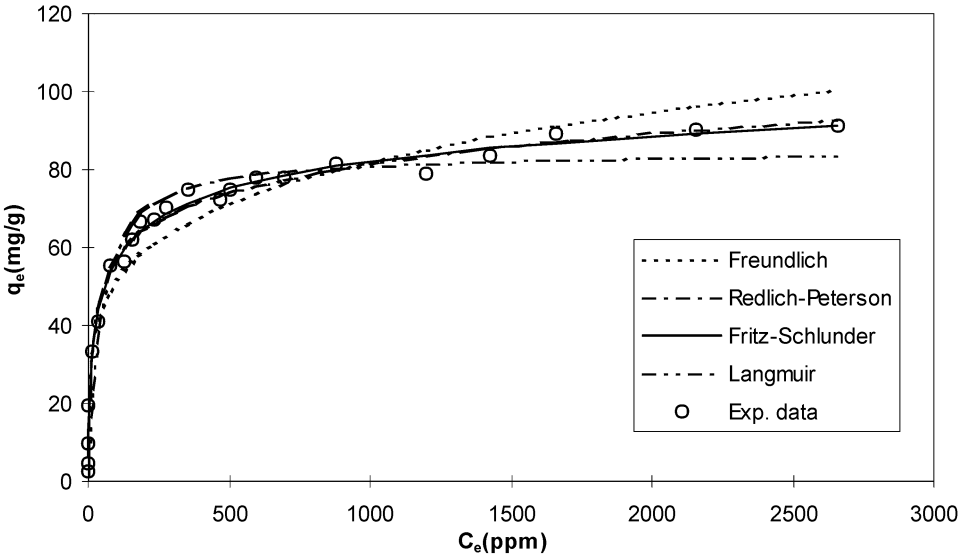

Fig. 2. Comparison of different equilibrium isotherm models for RN/F-400 system.

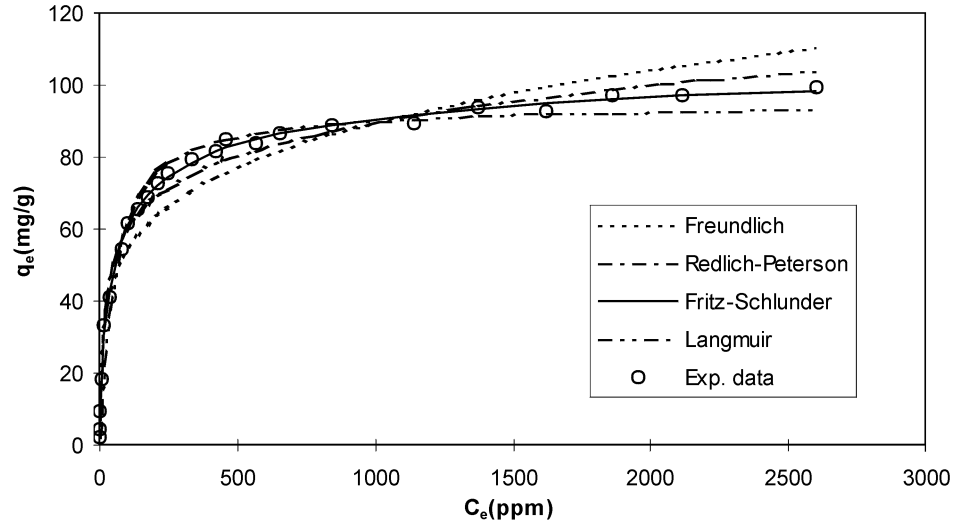

Fig. 3. Comparison of different equilibrium isotherm models for RR/F-400 system.

similar equilibrium behaviour, demonstrated by their relatively close k_s/a_s and q_{sat} values.

5.2. Kinetics study

In this work, the effects of initial concentration and particle size on the adsorption of reactive dyes on F-400 were investigated. For all experiments, the agitation speed was maintained constant at 400 rpm, the mass of activated carbon was 7.5 g and the solution volume was 2.5 l giving a solid/liquid ratio of 3.

5.3. Production of the concentration decay curves

Results of the BPDM application were presented in terms of the concentration decay curves, where the shape of the

Table 2
Parameter values from fitting the adsorption equilibrium data with Fritz–Schlünder isotherm

Adsorbate	Concentration range (mg/l)	k_s (mg/g)(mg/l)$^{-b_1}$	a_s (mg/l)$^{-b_2}$	b_1 (–)	b_2 (–)	k_s/a_s (mg/g)(mg/l)$^{b_2-b_1}$	q_{sat} (mg/g)
RR	0∼2600	5.51	0.0759	0.770	0.725	72.6	99.3
RY	0∼2177	1.61	0.0134	3.31	3.23	120	205
RN	0∼2650	9.23	0.180	0.717	0.639	51.3	91.4

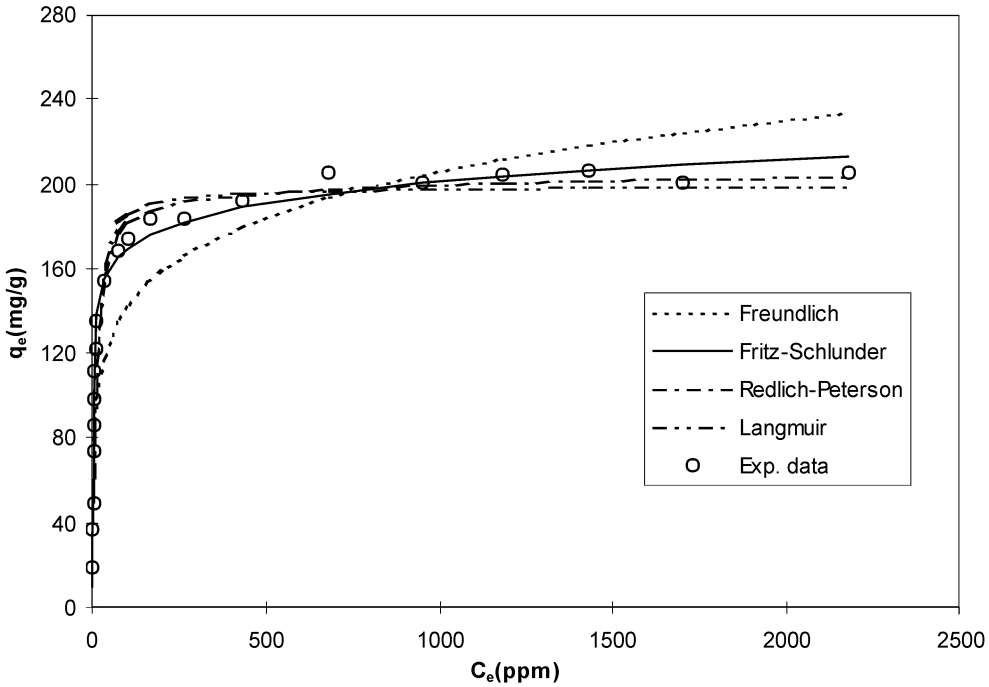

Fig. 4. Comparison of different equilibrium isotherm models for RY/F-400 system.

curve resulted from non-linear combination of the four mass transfer parameters mentioned earlier. Figs. 5–8 show a good agreement between experimental and theoretical data over 30 h of adsorption. Table 3 displays the mass transfer parameters that describe the theoretical results. It can be noticed that for k_f, k_b and f, a single value described each dye/carbon system for the whole experimental range while D_s varied with the initial dye concentration. This point will be further discussed in the following section.

As mentioned earlier, NAG routine E04JAF was incorporated in the computer program (developed earlier by McKay et al. [7]) to find the combination of parameters that best described the data. The objective function to minimise was the root mean square (RMS) of the normalised residuals:

$$\mathrm{RMS} = 100 \times \sqrt{\frac{1}{N}\sum_{i=1}^{N}\left(1 - \frac{q_{\mathrm{cal},i}}{q_{\mathrm{exp},i}}\right)^2} \quad (5)$$

Where N is the number of experimental points, $q_{\mathrm{exp},i}$ and $q_{\mathrm{cal},i}$ are the experimental and calculated solid-phase concentrations, respectively.

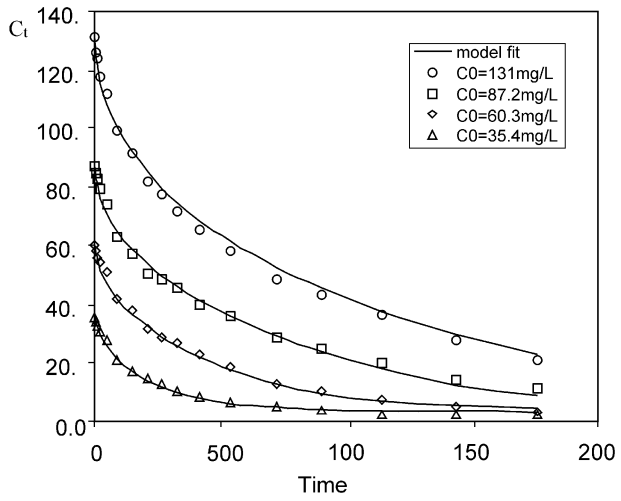

Fig. 5. Application of the BPDM to RY/F-400 system, using several initial dye concentrations.

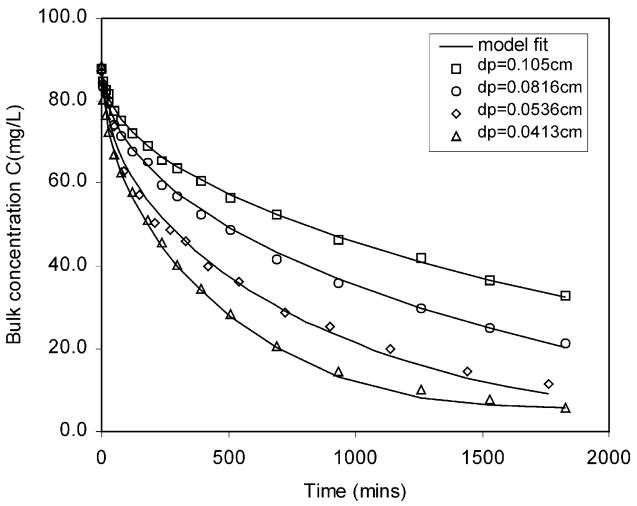

Fig. 6. Application of the BPDM to RY/F-400 system, using several sorbent particle sizes.

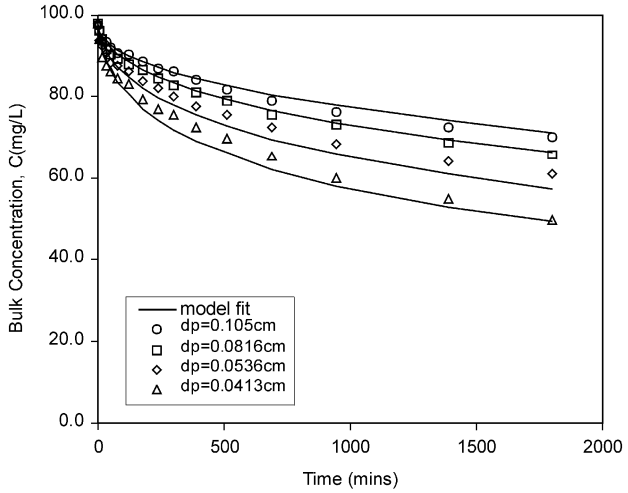

Fig. 7. Application of the BPDM to RR/F-400 system, using several sorbent particle sizes.

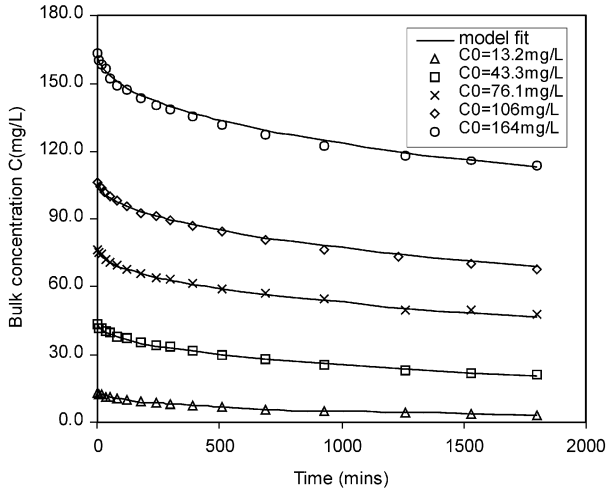

Fig. 8. Effect of initial concentration on the rate of RN adsorption on F-400 in a batch reactor.

5.4. Analysis of the mass transfer parameters

As mentioned earlier, an overall glance at Table 3 reveals that a single value of k_f, k_b and f described each dye/carbon system, while D_s increased with increasing the initial adsorbate concentration.

5.5. The external (film) mass transfer coefficient k_f

In this work k_f was evaluated by a single resistance assumption model, then adjusted during curve fitting [7]. Table 3 demonstrated that a single value of k_f described the whole range of system conditions. This would be expected as k_f is related to the thickness of the boundary layer and system hydrodynamics (such as solid/liquid ratio), which would be constant for a given system due to constant agitation speed, relatively narrow range of adsorbent size, and constant adsorbent mass employed in the experiments. Compared to other dyes, phenol and other benzene derivatives [11], Table 3 shows k_f to have much lower values. This was attributed to the size and the molecular structure of the present dyes. All the three reactive dyes consist of no less than four KeKular rings, with molecular weight ranging from 800 to 1100, thus the molecular motion would be

Table 3
Mass transfer parameters resultant from application of the BPDM to the systems under investigation

Run No.	Solute	C_0 (mg/dm^3)	d_p (cm)	$k_f \times 10^4$ (cm/s)	$D_s \times 10^{10}$ (cm^2/s)	$k_b \times 10^7$ (s^{-1})	f	RMS (%)
1	RY	35.4	0.0536	5.0	1.15	1.0	0.37	21
2	RY	60.3	0.0536	5.0	1.5	1.0	0.37	13
3	RY	87.2	0.0536	5.0	2.0	1.0	0.37	6.9
4	RY	131	0.0536	5.0	3.65	1.0	0.37	4.4
5	RY	88.4	0.0413	5.0	2.0	1.0	0.36	6.4
6	RY	87.9	0.0816	5.0	2.0	1.0	0.42	2.0
7	RY	87.9	0.105	5.0	2.0	1.0	0.42	1.02
8	RR	97.9	0.0413	5.0	4.0	4.0	0.40	3.2
9	RR	97.9	0.0536	5.0	4.0	4.0	0.38	2.9
10	RR	97.9	0.0816	5.0	4.0	4.0	0.40	0.92
11	RR	97.5	0.105	5.0	4.0	4.0	0.40	1.1
12	RN	13.2	0.0536	4.5	1.6	8.0	0.38	3.5
13	RN	43.3	0.0536	4.5	2.0	8.0	0.83	1.3
14	RN	76.1	0.0536	4.5	2.25	8.0	0.37	1.3
15	RN	106	0.0536	4.5	2.85	8.0	0.38	1.2
16	RN	164	0.0536	4.5	4.85	8.0	0.38	0.98
Reference								
[3]	Phenol	96.3	16 × 30 mesh	182	901	18.7	0.66	
[11]	Benzene	100	0.0428	200	80	70	0.30	
[11]	N-benz	100	0.0428	300	300	50	0.80	
[4]	BB69	106	0.0428	15	7.9	2.0	0.18	
[4]	BY21	103	0.0428	28	6.8	15	0.6	

considerably slower than that of benzene derivatives and basic dyes.

5.6. The micropore rate coefficient k_b

The adsorption mechanism in the micropores is strongly dependent on the pore geometry. The small diameter of the micropores makes their size comparable to the molecular diameter of the adsorbate molecules on the one hand, and promotes multidirectional interactions [12] on the other hand. In this work, the micropore rate coefficient k_b was evaluated by the NAG subroutine E04JAF mentioned earlier. Table 3 shows that k_b values are 1.0×10^{-7}, 4.0×10^{-7} and $8.0 \times 10^{-7}\ s^{-1}$ for RY, RR and RN, respectively. The difference in value between the three dyes of the same family was attributed to the difference in polarity and interactive nature of the dyes. RR and RN appeared to have larger molecules and be more polar (as they have more functional groups) than RY, the factor that enhanced the dye/pore-wall interactions. Also, compared to the k_b values of benzene derivatives and dyes on carbon, k_b for the present systems was much smaller. It must be mentioned here that the decreased pore radii in the micropores raise the energy barrier in the surface migration process, greatly reducing its rate. Also, the rate of micropore diffusion is a strong function of the solute diameter/pore diameter ratio [13,14]. In effect a ratio as low as 1:10 reduces the diffusion rate by 40%. Hence the large sizes of reactive dye molecules (compared to basic dyes and more prominently, benzene derivatives) would raise the solute/pore diameter ratio and would be expected to reduce the rate of diffusion, compared to the previously investigated systems.

5.7. Fraction of total adsorptive capacity in macropores f

As mentioned earlier, f is a parametric approximation of the fraction of the carbon particle adsorptive capacity that is occupied by macropores. Though apparently a structural property, the value of f depends on the properties of both adsorbate and adsorbent. For instance, 'large' adsorbate molecules encounter molecular sieving effects, and hence remain mainly in the macropores. In this work, results show that for RR and RN f was 0.40 and 0.38, respectively. For RY it averaged around 0.37 but increased by around 10% with carbon particle size. In comparison, dyes/Bagasse Pith systems showed f values of around 0.55, which suggested that Bagasse pith had smaller pore, forcing the dye to remain in the macropores. De-sorption studies would be required to confirm this.

$q_s(1 - f)$ gives the micropore adsorptive capacity. It is independent of the equilibrium behaviour and is due to the strong adsorbent affinity for adsorbates. For the present systems $q_s(1 - f)$ values were 59.6, 54.8 and 123 mg/g for RR, RN and RY, respectively. It was noticed that RY had the lowest k_b value yet the highest micropore capacity. The structures of these molecules (Appendix A) show that RY has the shortest molecule with no branches and lower polarity. This suggested that it would experience least multidirectional interactions (lowest k_b). On the other hand, due to the non-polar nature of the carbon surface, RY would be the most strongly adsorbed the factor that explains the high micropore capacity.

5.8. Surface diffusivity D_s

5.8.1. Effect of initial concentration C_0

Macropores are the inlet to the interior of adsorbent particles, and occupy most of the pore volume. Molecular transport in the macropores was described by the solid diffusion mechanism, measured by D_s, the solid diffusivity. Its value largely depends on the surface properties of adsorbents. For the present systems, the values of D_s shown in Table 3, fall well within the magnitudes reported in literature [15], specifically for chemisorption systems (10^{-5}–$10^{-13}\ cm^2/s$). However, compared to basic dyes and benzene derivatives on carbon, these values are much lower than those of benzene derivatives, and comparable with those of basic dyes. This was attributed to the large molecular size of the present systems, the factor that slows down the diffusion rate. In addition, the present molecules have more complex structures than benzene derivatives, and therefore their strong interactive nature with the carbon surface reduces their mobility.

Unlike previous papers on the BPDM, the present work yielded D_s values that increased with the initial solute concentration, without mathematical inconvenience. Such tendency was long established in literature [15] and attributed to the distribution of binding energies on heterogeneous surface [16]. At low coverage transport proceeds by the jumping of molecules between adjacent surface sites. At higher coverage neighbouring molecules interact and the process bears some similarity to liquid diffusion. However, the variation in D_s is due to progressive filling of sites of decreasing energy. This was all proved in chemistry research [17,18], yet it was never reported in literature as an outcome of the BPDM. The reason is the mathematical complexity of the BPDM, which was resolved in this paper. McKay and Al-Duri [4] described their systems of basic dyes/carbon with a single set of k_f, D_s, k_b and f, over a 24 h period.

The concentration dependence of D_s was related to the activation energy of the adsorption process. Gilliland et al. [8] correlated the surface diffusivity D_s to the heat of adsorption ΔH_{st}:

$$D_s = D_{s0} \exp\left(\frac{-\alpha \Delta H_{st}}{R_g T}\right) \tag{6}$$

By further assuming a linear relationship between ΔH_{st} and q at constant temperature, and introducing the solid-phase concentration at surface saturation q_{sat}, Eq. (6) becomes

$$D_s = D_{s0} \exp\left\{k\left(\frac{q}{q_{sat}}\right)\right\} \tag{7}$$

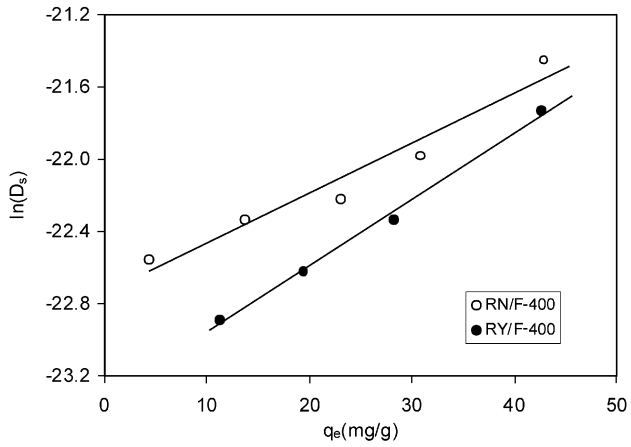

Fig. 9. D_s and q_e relationship for RN/F-400 and RY/F-400 system.

Eq. (7) has been successfully applied to the adsorption from dilute aqueous solutions [19,20]. In this work, D_s was correlated to q_s, the equilibrium solid concentration under the specified operating condition, and the results are presented in Fig. 9. It can be seen that there was a clear linear relationship between D_s and q_s for RY/F-400 system, though the linearity was not so prominent for RN/F-400 system.

An overall consideration of Table 3 shows that RY and RN have similar diffusive behaviour, yielding close D_s values, yet they have dissimilar equilibrium behaviours, indicated by the different affinity of carbon towards the two dyes. On the other hand, RR and RN have similar equilibrium patterns and carbon affinity, while they have dissimilar diffusive behaviour. RR is the fastest diffuser, while RY has the highest carbon affinity. Such findings would provide a good basis for investigation of multicomponent adsorption using the BPDM. Though attempted by the authors, the work still encounters mathematical difficulties and is not resolved yet. However, the film-solid diffusion model was successfully extended to multicomponent systems [21].

5.8.2. Effect of particle size

The effect of adsorbent particle size on D_s has received little attention compared with that of the solute concentration. Previous studies showed that D_s might either decrease [22], be invariant [16], or increase with increasing particle size exponentially [21].

In the present work, D_s was shown to be independent of particles size d_p for both RY/F-400 system and RR/F-400 system. However, Figs. 6 and 7 showed that for RR/- and RY/carbon systems, the overall rate increased as the particle size decreased. This could be attributed to the increase in the outer surface area of adsorbent of smaller particle size, which would result in a more rapid uptake of dye molecules. Meanwhile, reducing the particle size would makes the inner pores more accessible, but it would not change the internal structure of the carbon particles and the overall adsorbent capacity. This was confirmed by calculating the Biot number, which represented the ratio of internal to external resistance in the system. Table 4 showed that Bi_f increased with increasing d_p, indicating that the internal resistance increased with increasing particle size.

Table 4
Biot number for RY/F-400 and RR/F-400 system

d_p (cm)	Bi_f	
	RY/F-400	RR/F-400
0.0413	58.3	177
0.0536	74.8	230
0.0816	91.8	311
0.105	119	393

6. Conclusion

From the above analysis, the following can be concluded:

1. Fritz–Schlünder equilibrium isotherm proved to be the most accurate isotherm to incorporate in the BPDM, as it combined surface heterogeneity with irreversible properties.
2. The BPDM successfully provided theoretical prediction of the system kinetics, up to 30 h in a short computational time. By incorporating the NAG optimising routine E04JAF, it yielded more accurate data and D_s values that varied with the solute concentration, at no mathematical expense.
3. D_s was successfully described as an exponential function of the surface coverage q_s. A future recommendation is to incorporate the so-obtained function with the main model.

When all experimental results and modelling results were analysed simultaneously, it was found the solid-phase diffusion coefficient D_s obtained increased as initial concentration increased, while the other three parameters (k_f, k_b and f) in the model maintained constant.

Acknowledgements

The authors would like to thank the board of CVCP and the School of Chemical Engineering, University of Birmingham for their financial support.

Appendix A. Structures of dyes under investigation

The molecular structures are shown in Figs. 10–12. However, flame emission analysis with Corning-400 Flame Photometer revealed that it is mostly $–SO_3Na$ rather than $–SO_3H$ that is attached to the Kekuler ring. The molecular weight is

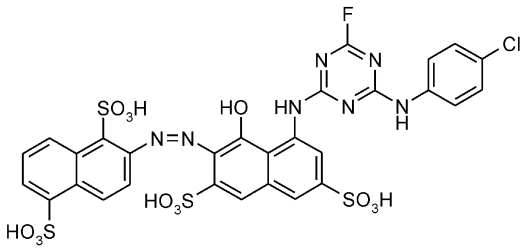

Fig. 10. Molecular structure of Cibacron Red F-B.

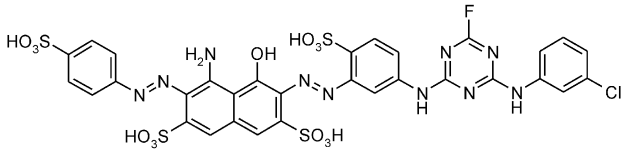

Fig. 11. Molecular structure of Cibacron Navy F-G.

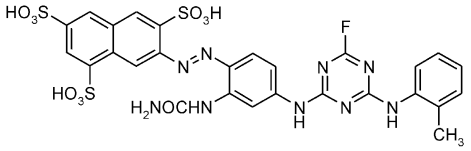

Fig. 12. Molecular structure of Cibacron Yellow F-3R.

Table A.1
Types and number of functional groups in reactive dyes

Functional groups (which accounts for polarity)	Number of functional groups		
	RY	RR	RN
$-SO_3Na$	3	4	4
−NH	2	2	2
$-NHCONH_2$	1	–	–
−F	1	1	1
−Cl	–	1	1
−OH	–	1	1
$-NH_2$	–	–	1

based on the SO_3Na. Table 5 displays the functional groups contained in the three reactive dyes.

References

[1] P. Cooper (Ed.), Colour in Dyehouse Effluent, The Alden Press, Oxford, 1995.

[2] A. Reife, H.S. Freeman (Eds.), Environmental Chemistry of Dyes and Pigments, Wiley/Interscience, New York, 1996.

[3] R.G. Peel, A. Benedek, C.M. Crowe, A branched pore kinetic model for activated carbon adsorption, AIChE J. 27 (1981) 26.

[4] G. McKay, B. Al-Duri, Branched-pore model applied to the adsorption of basic dyes on carbon, Chem. Eng. Process. 24 (1988) 1.

[5] J.S.J. Van Deventer, Kinetic model for the adsorption of metal cyanides on activated charcoal, Ph.D. Thesis, University of Stellenbosch, South Africa, 1984.

[6] S.P. Liebenberg, J.S.J. Van Deventer, The dynamic simulation of in-pulp sorption processes using the lumping of competitive and fouling phenomena, Min. Eng. 10 (1997) 959.

[7] G. McKay, S. McKee, H.R.J. Walters, Solid–liquid adsorption based on external mass transfer, macropore and micropore diffusion, Chem. Eng. Sci. 42 (1987) 1145.

[8] E.R. Gilliland, R.F. Baddour, et al., Diffusion on surfaces: I. Effect of concentration on the diffusivity of physically adsorbed gases, Ind. Eng. Chem. Fundam. 13 (1974) 95.

[9] W. Fritz, E.U. Schlünder, Simultaneous adsorption equilibria of organic solutes in dilute aqueous solution on activated carbon, Chem. Eng. Sci. 29 (1974) 1279.

[10] B. Al-Duri, A review in equilibrium in single and multicomponent liquid adsorption systems, Rev. Chem. Eng. 11 (1995) 101.

[11] Y. Sulaiman, The application of coconut shell activated carbon for water treatment: characterisation studies, Ph.D. Thesis, The University of Birmingham, Birmingham, UK, 1998.

[12] M.M. Dubinin, Porous structure and adsorption properties of active carbons, in: Chemistry and Physics of Carbon, Vol. 2, Marcel Dekker, New York, 1966.

[13] R.E. Beck, J.S. Schultz, Hindered diffusion in microporous membranes with known pore structure, Science 170 (1970) 1302.

[14] N. Wakao, T. Funazkri, Effect of fluid dispersion coefficients on particle-to-liquid mass transfer coefficients in packed beds, Chem. Eng. Sci. 33 (1978) 1375.

[15] D. Chazopoulos, A. Varma, R.L. Irvine, Activated carbon adsorption and desorption of toluene in the aqueous phase, AIChE J. 39 (1993) 2027.

[16] A.P. Mathews, I. Zayas, Particle size and shape effects on adsorption rate parameters, J. Environ. Eng. 115 (1989) 41.

[17] Y. Sudo, D.M. Misic, M. Suzuki, Concentration dependence of effective surface diffusion coefficients in aqueous phase adsorption on activated carbon, Chem. Eng. Sci. 33 (1978) 1287.

[18] B. Al-Duri, G. McKay, Prediction of binary system for kinetics of batch adsorption using basic dyes onto activated carbon, Chem. Eng. Sci. 46 (1991) 193.

[19] K. Miyabe, S. Takeuchi, Model for surface diffusion in liquid-phase adsorption, AIChE J. 43 (1997) 2997.

[20] I. Neretnieks, Analysis of some adsorption experiments with activated carbon, Chem. Eng. Sci. 31 (1976) 1029.

[21] B. Al-Duri, Mass transfer processes in single and multicomponent batch adsorption systems, Ph.D. Thesis, The Queen's University of Belfast, Northern Ireland, 1988.

[22] D.M. Ruthven, Principles of Adsorption and Adsorption Processes, Wiley, New York, 1984.